

SPATIAL DISTRIBUTIONS OF THE EMITTING SPECIES IN A PENNING SURFACE-PLASMA SOURCE*

H. Vernon Smith, Jr., Paul Allison, Kourosh Saadatmand,** and J. David Schneider
Los Alamos National Laboratory, Los Alamos, NM 87545 USA

Abstract

Using optical spectroscopy we study the spatial and temporal distributions of the H_{α} , CsI(4555 Å), CsII(4604 Å), and MoI(3903 Å) emission lines in a Penning surface-plasma source (SPS). A diagnostic slit exposes the entire SPS discharge gap either parallel or perpendicular to the magnetic field. The spatial and temporal distributions of the emitting species are recorded using a 1-m monochromator. The visible light and the H_{α} and CsII(4604 Å) spatial distributions are also recorded with a video camera. The cesium atomic and ionic light, and the molybdenum atomic light, is strongly concentrated near the cathodes; the visible light and the H_{α} light is almost uniform in both directions. These measurements are presented and discussed.

Introduction

To continue our studies of the Penning SPS source, we recently constructed and began testing the 8X Source. It has about twice the linear dimensions of the 4X Source.¹ The spatial distributions of the visible light emitted through a diagnostic slit, recorded with a video camera, indicate increased light emission at the cathodes. By placing a wide-band-pass monochromator in front of the video camera to filter out the other lines the light from the H_{α} and CsII(4604 Å) lines is also recorded. The spatial distribution and time evolution of several visible emission lines are also studied using a 1-m monochromator. Another study of the spatial and temporal distributions of the light emitted from a similar Penning SPS is reported in Ref. 2.

Experimental Method

As shown in Fig. 1, the 0.64 mm wide \times 3.7 cm long diagnostic slit exposes a narrow strip of the discharge from cathode to cathode when it is oriented parallel to the magnetic field (3.4 cm cathode-cathode gap); it exposes a narrow strip from anode to anode when it is oriented perpendicular to the field (3.4 cm anode-anode gap). The area of the diagnostic slit nearly equals the area of the 5.4-mm-diam circular emitter for H^{-} beam extraction.

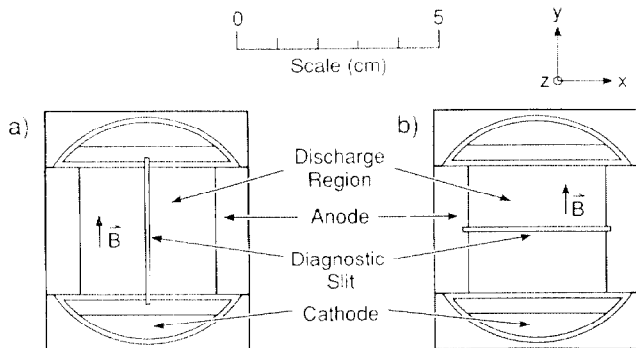


Fig. 1. Diagnostic slit aligned a) along the y direction from cathode to cathode or b) along the x direction from anode to anode.

A model 4815-2000 video camera manufactured by Cohu, Inc., equipped with a 200 mm Nikon lens, is used to measure the light emitted through the diagnostic slit (Fig. 2a). The video camera frame rate is 30 frames/s; the video camera detector is a CCD device with 30 ms integration time, so all of the light emitted in a single pulse is summed (the arc pulse length is \approx 1 ms, the arc repetition rate is 5 Hz). The video camera is controlled by an IBM AT microcomputer. The microcomputer stores the video camera images of the diagnostic slit (typically 10 lines high by 600 pixels wide) in 30 line by 720 pixel arrays for further analysis. The video camera is carefully oriented so that the long axis of the slit image is parallel to the 720-pixel axis of the video camera. Irregularities in the diagnostic slit are avoided by examining only the pixels in the center line of the slit image.

* Work supported by the US Department of Defense, US Army Strategic Defense Command under auspices of the US Department of Energy.

** Grumman Corporate Research Center, Bethpage, NY 11714 USA

A SPEX model 1704 1-m monochromator is used as a narrow-band filter to study the optical emission of the hydrogen atoms (with the H_{α} and H_{β} Balmer lines), cesium atoms (the CsI line at 4555 Å), cesium ions (the CsII line at 4604 Å), and molybdenum atoms (the MoI line at 3903 Å). The experimental arrangement for the cathode-cathode measurements is shown in Fig. 2b. One mirror (M_4) in a four-mirror arrangement is mounted on a micrometer-driven table. This arrangement allows the diagnostic slit image, formed by the lens L_1 (focal length = 30 cm), to be moved across the monochromator entrance slits (set at 0.10 mm separation). The four-mirror system is rotated 90° about a horizontal axis for the anode-anode measurements (not reported here). At each M_4 position the light intensity traversing the monochromator is measured with a photomultiplier tube (PMT). The time spectrum of each line is recorded at the discharge center and at the peak of the cathode light emission by moving M_4 to the appropriate location and taking an oscillogram of the PMT signal.

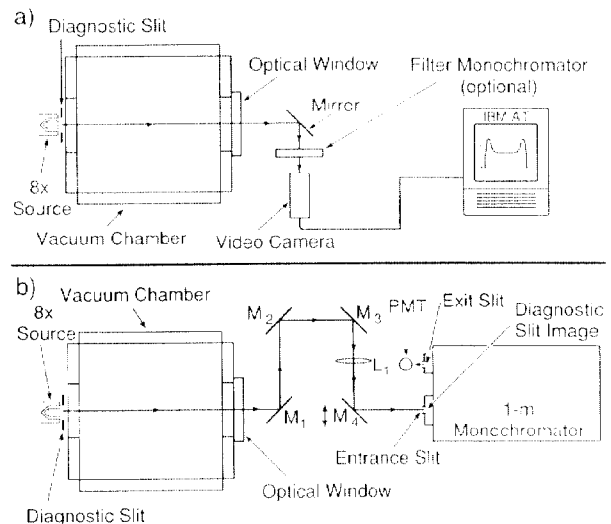


Fig. 2. a) Schematic of the video camera cathode-to-cathode light intensity measurements. For the anode-to-anode measurements, the diagnostic slit and the video camera are rotated 90° about the light axis. A filter monochromator is placed in front of the video camera to record the spatial distributions of the H_{α} and CsII(4604 Å) lines. b) Schematic of the 1-m monochromator, cathode-cathode, line-intensity distribution measurements.

We know from previous measurements of the 4X source discharge³ that the H_{α} line is the most intense line in the spectrum. In addition, it is several hundred angstroms away from the nearest line of any appreciable strength. Thus, we recorded the H_{α} line intensity distribution by placing a filter monochromator (Oriel model 7155 Filter Monochromator) in front of the video camera and tuning it to 6560 Å (Fig. 2a). This technique also works for the CsII(4604 Å) line.

Results

The video camera data for the cathode-cathode and anode-anode light distributions are shown in Figs. 3a and 3b, respectively. We calibrated the abscissae in separate measurements. For the 2 A DC discharge the total light emitted is very uniform cathode to cathode (with the exception of the near-cathode region), but it is nonuniform anode to anode (peaked at the center of the discharge). For the 450 A pulsed discharge the total light emitted is very uniform anode to anode (with the exception of the near-anode region), but it is nonuniform cathode to cathode (peaked near the cathodes).

The 1.1- μ s-long, 5 Hz discharge voltage and current waveforms, and the time spectra for the hydrogen, cesium, and molybdenum lines at the peak of the cathode emission, are shown in Fig. 4. Hydrogen gas and cesium vapor are purposely added to the discharge. Molybdenum is sputtered from the cathodes into the discharge. The turn-on transient in the discharge voltage V_d and discharge current I_d lasts \approx 150 μ s. The voltage V_d goes through a maximum of \approx 300 V before stabilizing at 120 V for the last 0.8 ms of the pulse whereas I_d

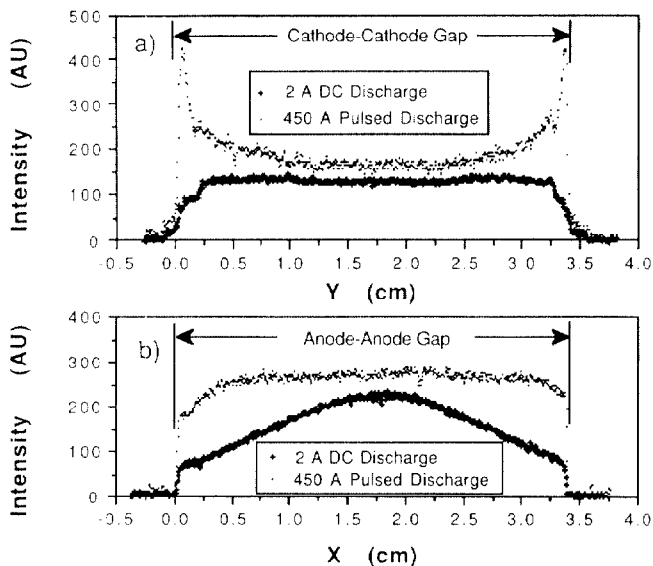


Fig. 3. Emitted light distributions for a 2 A DC discharge (crosses) and a 450 A pulsed discharge (points) along a) the y direction or b) the x direction. The cathode surfaces are at $y = 0$ and 3.4 cm; the anode surfaces, at $x = 0$ and 3.4 cm.

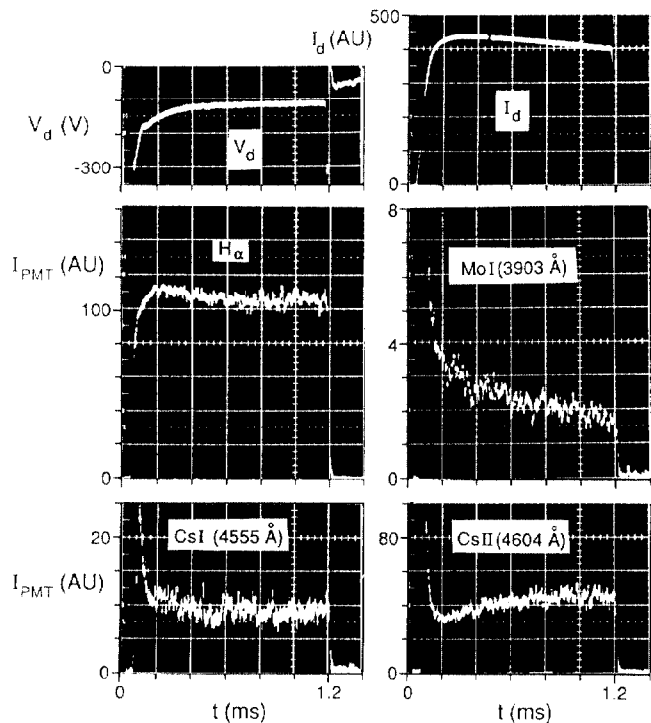


Fig. 4. The discharge voltage V_d and discharge current I_d for the 8X source pulsed discharge are shown in the upper oscillograms. Below them are the time spectra for the H_α , CsI(4555 Å), CsII(4604 Å), and MoI(3903 Å) emission lines at the peak of the light emission near the cathode surface ($y = 0.1$ cm).

peaks at ≈ 450 A before decaying away to 400 A at the end of the pulse. The light emission at the end of the pulse (at $t=1.2$ ms in the Fig. 4 oscillograms) is plotted in Figs. 5 and 6. The video camera data plotted in Figs. 3 and 6 are integrated by the CCD detector in the camera over the whole 1.1-ms-long discharge pulse.

The CsII(4604 Å) line intensity distribution for a 120 V, 400 A pulsed discharge from cathode to cathode (Fig. 5) peaks near the cathodes. Provided the excitation probability to the emitting state of the Cs ions is spatially independent, the distribution of the Cs ion emission reflects the distribution of the Cs ions. If this is the case, then the Cs ion density is ten times higher near the 8X source cathodes than at the discharge center. A similar conclusion can be reached for the cesium and molybdenum atom distributions for the pulsed discharge, but the

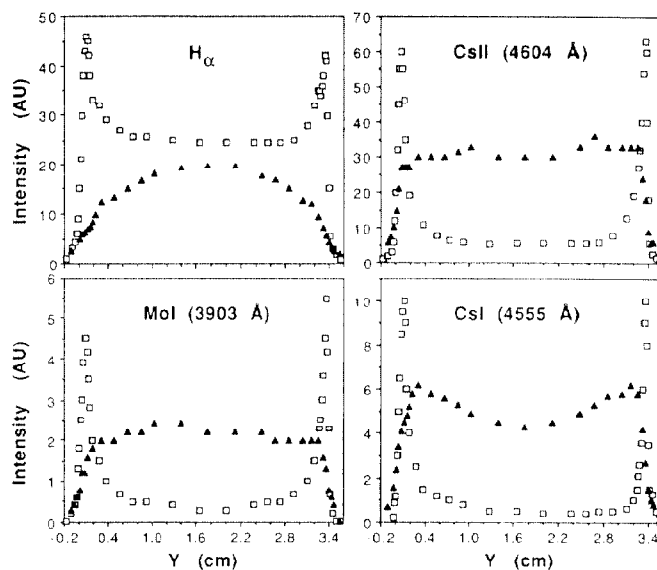


Fig. 5. Emission line distributions from cathode to cathode for hydrogen atoms (H_α), cesium atoms [CsI(4555 Å)], cesium ions [CsII(4604 Å)], and molybdenum atoms [MoI(3903 Å)] measured with the 1-m monochromator. The 120 V, 400 A pulsed discharge data are the open squares; the 72 V, 2 A DC discharge data, the filled triangles. The cathode surfaces are at $y = 0$ cm and $y = 3.4$ cm.

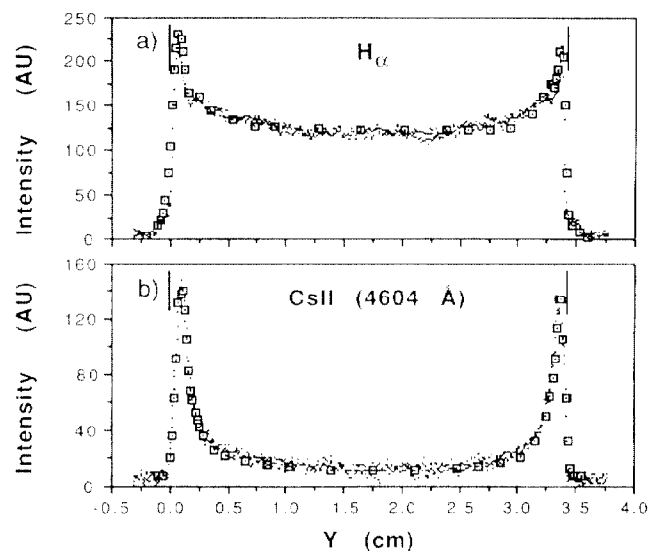


Fig. 6. a) The emitted H_α light cathode to cathode recorded with the video camera through the filter monochromator tuned to 6600 Å (dots) and the 1-m monochromator (squares). The 1-m monochromator data are adjusted to make the peak locations and average peak heights the same as in the video camera measurement. b) The emitted CsII(4604 Å) light cathode-to-cathode (the filter monochromator is tuned to 4600 Å). Otherwise the same as a).

hydrogen atom distribution is more nearly uniform, with at most a 2:1 density ratio between the cathode and mid-arc regions (Fig. 5).

The line intensity distributions from cathode to cathode for a 72 V, 2 A DC discharge are also shown in Fig. 5. These profiles are very different from the pulsed case, as we know they must be from the video camera work (see Fig. 3). Now the H_α emission is maximum at the discharge center and the CsII(4604 Å) and MoI(3903 Å) emission is nearly uniform from cathode to cathode. The CsI(4555 Å) emission still has peaks, but these maxima are now ≈ 2 mm from the cathode. Possibly this indicates a much wider cathode sheath for the 2 A DC discharge than for the 400 A pulsed discharge (see below).

Figure 6a shows the spatial distribution of the H_α light recorded with the video camera when the filter monochromator is placed in front of the video camera (Fig. 2a) and tuned to pass the H_α emission light. The filter monochromator has a half-width at half-maximum of

$\sim 200 \text{ \AA}$ at the H_α wavelength of 6562.8 \AA . From previous work with the 4X source³ we know that the H_α line is the strongest emission line in the spectrum, and that the spectrum is clear of all but very weak lines 600 \AA on either side of H_α . Thus, the light transmitted through the filter monochromator to the video camera is dominated by H_α . In Fig. 6a the 1-m monochromator data from Fig. 5 are placed on the video camera measurements for H_α . The agreement between the two data sets is very good, especially since the video camera and the 1-m monochromator measurements were taken 13 days apart.

The intense CsII line at 4604 \AA is well-separated from other strong emission lines; the emission lines that are within $\pm 300 \text{ \AA}$ of it are either weak CsII lines or the weak CsI line at 4555 \AA (Ref. 3). Thus, tuning the filter monochromator to 4600 \AA and recording the CsII (4604 \AA) line with the video camera gives the spatial distribution shown in Fig. 6b. Data from the CsII(4604 \AA) 1-m monochromator measurements are also shown in Fig. 6b. The agreement between the two data sets is very good. The 1-m monochromator measurements take about 1 h for each data set, whereas each video camera set takes about 1 min. Thus, the filter monochromator-video camera technique is quick as well as accurate for well-isolated, intense emission lines. For closely spaced or weak lines, the high-wavelength resolution of the 1-m monochromator technique is needed.

Discussion

If the emitted discharge light intensity is an accurate measure of the plasma density, non-uniform light emission would indicate a non-uniform power loading on the 8X source electrodes. If the discharge nonuniformity were severe enough, the ion optics of the extracted H^- beam could be seriously degraded by nonuniformities of the H^- density across the emission surface. For the 450 A pulsed discharge the light emission is uniform anode to anode. It is also uniform cathode to cathode, with the exception of the near-cathode region. However, the peaks in the cesium and molybdenum light emission near the cathodes are certainly associated with processes in the discharge which affect the cathodes. Note that in all cases the discharge is fairly uniform at mid arc within the size of the 5.4-mm-diam emitter for H^- beam extraction. The conclusion reached from the video camera results of Fig. 3 is that both the 8X source power loading and the H^- emission current density are expected to be uniform.

We expect the 8X source discharge electron density and temperature to be uniform cathode to cathode because the magnetic field is strong enough ($\sim 0.05 \text{ T}$) to confine the electrons to trajectories parallel to the field. The electron density and temperature may be nonuniform anode to anode because the electron diffusion coefficient perpendicular to the magnetic field is « the electron diffusion coefficient parallel to the magnetic field. We make the assumption that the processes which produce the observed decaying atomic and ionic excited states, such as electron-impact ionization, are spatially independent, and that the emission line intensities are directly proportional to the density of the emitting species. If this is true, the CsI(4555 \AA), CsII(4604 \AA), and MoI(3903 \AA) emission line distributions in Fig. 5 mean that the Cs^0 , Cs^+ , and Mo^0 densities are much larger near the cathode than at mid-arc for the 400 A pulsed discharge.

The temporal behavior of the hydrogen, cesium, and molybdenum light emission for the near-cathode region is shown in Fig. 4. During the discharge pulse turn-on transient, the CsI(4555 \AA), CsII(4604 \AA), and MoI(3903 \AA) emission lines have narrow (in time) peaks. After the transient, the CsI(4555 \AA) emission is constant, but there is a slight increase in the CsII(4604 \AA) emission and a larger decrease in the MoI(3903 \AA) emission. Near the cathodes, the H_α emission is remarkably constant throughout the whole pulse. When the discharge turns on, the cesium residing on the cathode surface is blown off, then ionized and trapped near the cathode. The sharp peak in the molybdenum emission probably corresponds to the high sputtering rates at the high discharge voltages during the turn-on transient. When the discharge voltage returns to $\approx 120 \text{ V}$, the molybdenum sputtering drops to much lower values than at 300 V . For the H_α peak near the cathodes the explanation is not so clear cut. Possibly hydrogen is transported to the cathodes, or perhaps we are seeing indirect evidence for H^- ions coming off of the cathode — perhaps the H_α peaks at the cathodes come from H^- ions undergoing mutual neutralization collisions with H^+ , leaving the H^0 in the $n=3$ state, which then decays giving off Balmer α light.

The variation of line intensities between cathodes (Fig. 5) suggests a tendency for species to be concentrated near the cathodes, because the density of electrons is presumably fairly uniform along the

magnetic field lines. For cesium, the mechanism is probably ionization of atoms sputtered from the cathodes and the subsequent return of the ions to the cathodes by residual plasma fields. From the CsI(4555 \AA) data in Fig. 5 the mean free path λ is estimated to be 16 mm and 0.43 mm for Cs^0 in the 2-A and 400-A discharges, respectively. For $kT_e < 2 \text{ eV}$ and a fast electron fraction $n_{fe}/n_e \approx 3\%$ with energies distributed uniformly up to 100 eV , the ionizing contribution of thermal electrons can be neglected. We use $\lambda = v_{Cs}/n_{fe} \langle \sigma v_e \rangle$, where v_{Cs} is the Cs atom velocity and $\langle \sigma v_e \rangle$ is the reaction rate. Putting in reasonable numbers for $\langle \sigma v_e \rangle$ [$3.6 \times 10^{-7} \text{ cm}^3/\text{s}$ (Ref. 4)] and v_{Cs} [$kT_{Cs} = 0.1 \text{ eV}$ (Ref. 5)] we get $n_e = 2 \times 10^{12} \text{ cm}^{-3}$ for the 2-A discharge and $n_e = 8 \times 10^{13} \text{ cm}^{-3}$ for the 400-A discharge. The plasma densities have not been measured for the 8X source, but these 8X source values are about as expected from the 4X source values in Ref. 6. Even though we estimate the Cs density in the absence of a discharge to be roughly 10^{-3} that of H_2 , the fraction of cathode current may be substantially larger because of the cathode concentration effect. The data of Fig. 5 also support the conjecture that if the source were to be run in a high-current DC mode, then the Cs^0 flow through the emission aperture would be greatly reduced from that for the pulsed case⁵, because the CsI intensity is ≥ 20 times greater at the cathodes than near the emission aperture; also, for pulsed operation of a Penning SPS most of the Cs^0 emission occurs in between the discharge pulses (Ref. 5).

The data in Fig. 5 may imply that the cathode sheath has a measurable size. For the 2 A DC discharge the CsI(4555 \AA) line intensity peaks 2 mm from the cathode surface; for the 400 A pulsed discharge it peaks about 0.05 cm from the cathode. We calculate a 0.005 cm sheath thickness for the 400 A pulsed discharge and 0.06 cm for the 2 A DC discharge. The agreement between the calculated and the measured sheath thickness for the 2 A DC arc is only fair. The factor of 10 disagreement between the measured and calculated sheath thickness for the 400 A pulsed discharge is not understood.

Under the 400-A plasma conditions, the ratio of plasma to neutral collision frequencies for the electrons is about 180, so we may neglect the contribution to diffusion by neutral collisions. Because the diffusion coefficient then depends on the plasma density, we expect better plasma confinement at lower density, and this would lead to a density buildup in the center of the discharge, as observed in Fig. 3b. A MHD model of electron diffusion predicts the features of low- and high-current density, but at much lower magnetic fields than 370 G . The neutral species except H_2 tend to stick or recombine at the walls and, therefore, their production and diffusion in the discharge volume may also lead to nonuniform distribution, as is the case for Cs for example. We expect that the optical emission generally reflects the distribution of fast electrons, but at the present this cannot be proved.

Summary

Based on the optical emission of the 8X source pulsed discharge, the cathode and the anode power loadings are expected to be uniform. The Cs^0 , Cs^+ , and Mo^0 distributions are fairly uniform from anode to anode, but all three are strongly peaked near the cathodes. After sputtering from the cathodes Cs^0 and Mo^0 presumably are trapped near the cathodes because their mean free paths for ionization are short; residual plasma fields return the resulting Cs^+ to the cathodes. The measured Cs^0 mean free paths are $\lambda = 0.43 \text{ mm}$ for the 400 A pulsed discharge and $\lambda = 16 \text{ mm}$ for the 2A DC discharge. By comparison with Cs^0 , Cs^+ , and Mo^0 , the H^0 distributions are uniform in both directions.

References

- [1] H.V. Smith, Jr, P. Allison, and J.D. Sherman, IEEE Trans. Nucl. Sci. NS-32 (1985), pp. 1797-9.
- [2] V.V. Antsiferov, V.V. Beskorovaynyy, A.M. Maximov, P.G. Sova, L.P. Skripal', Yu.I. Belchenko, and G.E. Derevyankin, "Spectroscopic Study of Hydrogen-Cesium Discharge Plasma of Surface-Plasma Ion Sources," AIP Conf. Proc. (1990) [to be published].
- [3] H.V. Smith, Jr., "Emission Spectroscopy of the 4X Source Discharge," Los Alamos National Laboratory report no. AT-2: Technical Note: 89-07.
- [4] P.W. van Amersfoort, "Formation of Negative Ions on a Metal Surface," Ph.D. thesis, University of Amsterdam, 1987.
- [5] H.V. Smith, Jr. and P.W. Allison, IEEE Trans. Nucl. Sci. NS-26 (1979), pp. 4006-8.
- [6] H.V. Smith, Jr., P. Allison, and R. Keller, AIP Conf. Proc. No. 158 (1987), pp. 181-92.